Molecular Crystals and Liquid Crystals
Publication details, including instructions for authors and subscription information:
http://www.tandfonline.com/loi/gmcl16

Low-Frequency Vibrational Spectrum of the Paratoluidine Single Crystal

N. Abasbegović [a] & L. Colombo [b]
[a] Department of Physics, University of Sarajevo, Yugoslavia
[b] Institute "Rudjer Bošković", Zagreb, Yugoslavia
Version of record first published: 21 Mar 2007.

To cite this article: N. Abasbegović & L. Colombo (1975): Low-Frequency Vibrational Spectrum of the Paratoluidine Single Crystal, Molecular Crystals and Liquid Crystals, 31:1-2, 53-67

To link to this article: http://dx.doi.org/10.1080/15421407508082858

Mol. Cryst. Liq. Cryst., 1975, Vol. 31, pp. 53–67

Printed in Holland

Low-Frequency Vibrational Spectrum of the Paratoluidine Single Crystal

N. ABASBEGOVIĆ

Department of Physics, University of Sarajevo, Yugoslavia

and

L. COLOMBO

Institute "Rudjer Bošković", Zagreb, Yugoslavia

(*Received November 13, 1974: in final form February 19, 1975*)

The lattice vibrational spectrum of the paratoluidine single crystal has been studied by Raman and IR spectroscopic techniques and calculated using the rigid-molecule approximation. Intermolecular interactions have been described taking into account the interactions between all types of atom pairs at interatomic distances smaller than 4.0 Å. The Raman spectrum has been measured at room and liquid-nitrogen temperatures. Forty lines have been observed at room temperature and the frequencies for 7 additional lines have been extrapolated from the spectrum recorded at low temperature. Twenty lattice vibrations have been observed in the far-infrared spectrum at 34 K. An assignment of the observed to the calculated frequencies has been proposed.

INTRODUCTION

Paratoluidine belongs to lattices with a relatively large number of molecules forming two sets of crystallographically independent units. The present investigation was undertaken with the aim of obtaining further information about the dynamics and intermolecular forces in such systems.

In an earlier experimental study of the lattice dynamics of the paratoluidine crystal[1] the experimental conditions realized by use of a mercury lamp were not sufficiently adequate to obtain a complete vibrational spectrum.

In the present work polarization measurements were performed on an oriented sample by the methods of laser Raman spectroscopy. Spectra were taken at room and liquid-nitrogen temperatures. In addition, the far-infrared spectrum of the oriented sample was measured at 34 K.

The most suitable method for describing lattice modes is the rigid-molecule approximation, as modified by Shimanouchi.[2]

Crystal structure and selection rules

Paratoluidine crystallizes in the orthorhombic system, space group $P_{na2_1}(C_{2v}^9)$, with eight differently oriented molecules in the unit cell.[3] (The dimensions of the unit cell are $a = 9.02$, $b = 6.0$, $c = 23.31$ Å.) According to the International Tables for X-Ray Crystallography[4] the space group C_{2v}^9 has four "general positions". The molecules are separated into two crystallographically independent sets (Set I and Set II). Figure 1 shows the arrangement of the molecules in the unit cell. The full lines represent the molecules forming Set I, while the dotted lines show the molecules forming Set II.

Since the molecules in both sets have the same site symmetry (C_1), they should satisfy the same selection rules defined by the group-theory treatment. From the correlation between the point and factor groups and taking into account the "general positions" of the molecules, it follows that each external motion of an individual molecule is present in each symmetry species of the factor group. The correlations between the point, site, and the factor groups are shown in Table I. In Table I are given the results of the group theory analysis for external motions of molecules in the crystal, and selection rules for the Raman and IR spectra.

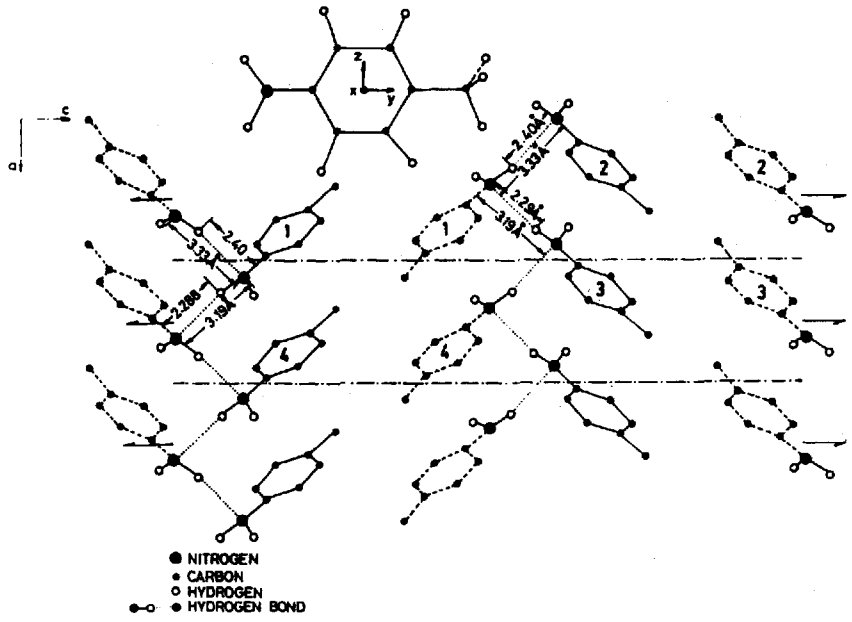

FIGURE 1 Molecular and crystal structure of paratoluidine; (010) projection. The molecules drawn in the full lines form Set I, those of dotted lines belong to Set II. X, Y, Z are the axis of inertia of the molecule.

TABLE I

Point Group, Site Group, and Factor Group Correlations

Point group C_s	Site group C_1	Factor group C_{2v}					
		R_j	T_i	T_i'	T_{acoust}	IR	R
$A'(R_x, T_y, T_z)$ $A''(R_y, R_z, T_x)$	A	A_1 $2(R_x, R_y, R_z)$	$2(T_a, T_b)$	T_c'	T_c	M_c	$\alpha_{aa}, \alpha_{bb}, \alpha_{cc}$
		A_2 $2(R_x, R_y, R_z)$	$2(T_a, T_b, T_c)$	—	—	f	α_{ab}
		B_1 $2(R_x, R_y, R_z)$	$2(T_b, T_c)$	T_a'	T_a	M_a	α_{ac}
		B_2 $2(R_x, R_y, R_z)$	$2(T_a, T_c)$	T_b'	T_b	M_b	α_{bc}

T_i—translational motions of molecules in a set
T_i'—translational motions of two sets against each other
R_j—rotational motions of molecules about the inertial axes
T_{acoust}—acoustic modes

The total irreducible representation of external vibrations is

$$\Gamma(\text{vibr}) = 12A_1 + 12A_2 + 12B_1 + 12B_2.$$

The two sets of molecules in the lattice imply the existence of two types of optical translational modes: Translational vibrations of molecules in each set are given by the irreducible representation

$$\Gamma(\text{OT}) = 4A_1 + 6A_2 + 4B_1 + 4B_2,$$

and the irreducible representation of translations with two sets of molecules moving rigidly against each other is

$$\Gamma(\text{OT}') = 1A_1 + 1B_1 + 1B_2.$$

The irreducible representation of optical librational modes is given by

$$\Gamma(\text{OR}) = 6A_1 + 6A_2 + 6B_1 + 6B_2.$$

The acoustic modes of this lattice are

$$\Gamma(\text{acoustic}) = 1A_1 + 1B_1 + 1B_2.$$

All 45 lattice vibrations are active in the Raman spectrum and 33 of them are active in the IR spectrum.

EXPERIMENTAL

Single crystals of paratoluidine were grown from the melt by Bridgman's method of very slow cooling. The preparation and conservation of oriented samples were rather difficult because of the low melting point (45°C) and the easy cleavage along the (001) plane. However, we were able to obtain some samples of sufficiently good size and quality. The orientation of the optical

axis in the sample was determined by means of isogyre patterns in a polarizing microscope. Raman spectra of single crystals were recorded in the region from 10–200 cm^{-1} by four different monochromators—Cary 81, Coderg PHO, DFS 12, and Coderg T 800 triple monochromator. The spectra were excited by argon ion laser (Coherent Radiation Type B 52 or Spectra Physics Model 165 03).

Polarized Raman spectra of a single crystal were taken at room and liquid-nitrogen temperatures. Raman spectra of powder samples were recorded at various temperatures ranging from 30 K to room temperature. The small number of measurements performed on powder samples at each temperature did not allow the determination of the frequency abberation for the observed bands. The errors in measurement are given only for room and liquid-nitrogen temperatures. The results of low-temperature measurements are shown in Figure 2. Because of the large number of bands, the curves describing the frequency dependence on temperature are represented for each symmetry species separately (Figures 2a, b, c, d). Some of the lines could be recorded only at low temperatures. Their frequencies at room temperature were derived by approximate extrapolation. In this way the bands $\sim 143\ (A_2)$, $\sim 143\ (B_1)$, $\sim 144\ (B_2)$, $\sim 144\ (A_1)$, $\sim 138\ (B_1)$, $\sim 138\ (B_2)$, and $\sim 55\ (B_2)\ cm^{-1}$ were obtained, as can be seen in Figure 2. The symmetry of the frequencies obtained by extrapolation was determined on the basis of measurements at liquid-nitrogen temperature.

Figure 3 shows a selection of Raman spectra recorded at room temperature. A notation similar to that of Damen *et al.*[5] was used. The far-infrared spectrum of a single crystal was measured at 34 K using a Grubb–Parson spectrometer. Only two orientations were measured because of the difficulty in preparing the sample. The results of these measurements are given in Table II.

Normal-coordinate analysis

We performed a normal-coordinate analysis for the paratoluidine crystal in order to assign the observed frequencies and to give a description of the lattice dynamics. The calculations were performed in the rigid-molecule approximation on a Univac 1106 digital computer, using a Fortran program written in our laboratory for similar studies.[6]

In our normal-coordinate treatment we used a model in which van der Waals and repulsion forces were expressed as a sum of all nonbonded atom–atom pair potentials. The potential function for two nonbonded atoms located at positions $\mathbf{r}_i$ and $\mathbf{r}_j$ is assumed to be

$$V(r_{ij}) = A\, e^{-\alpha r_{ij}} - \mathrm{Br}_{ij}^{-6},$$

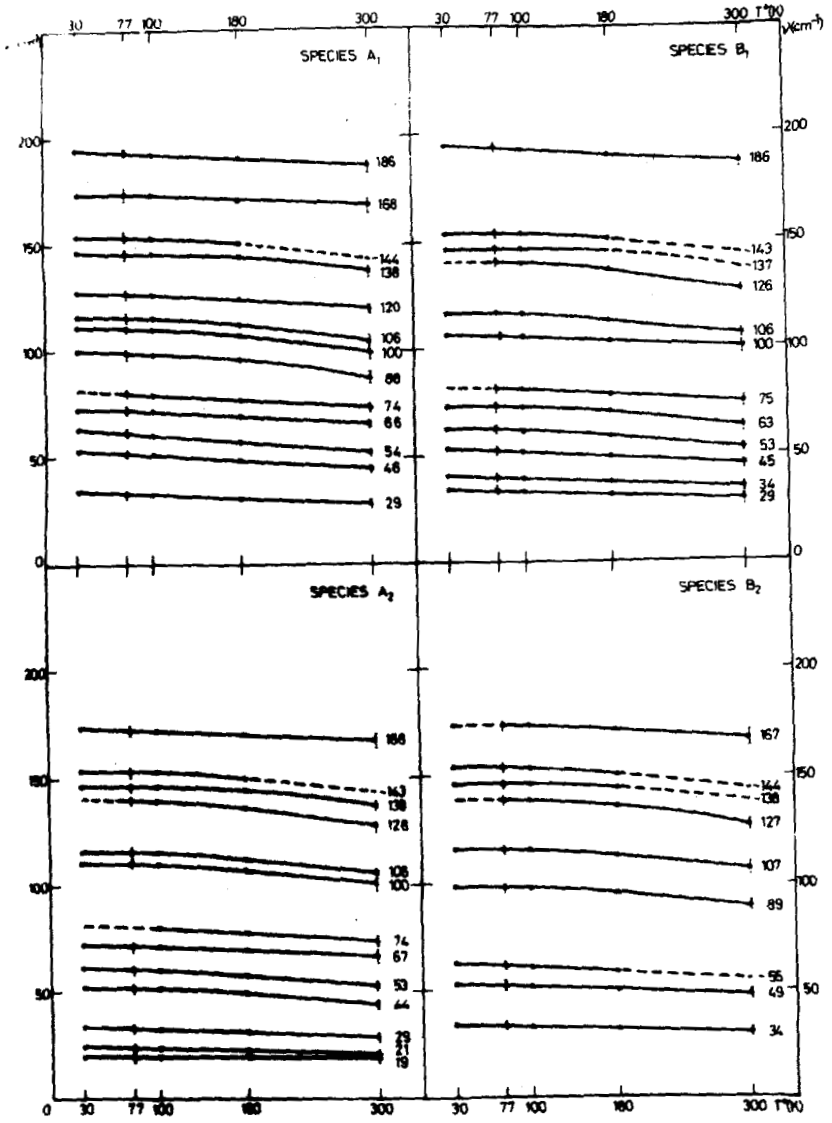

FIGURE 2 Frequency dependence on temperature.

TABLE II

The observed and calculated spectra

Species	Observed Raman 300°K	Observed Raman 77°K	Observed Fir 34°K	Calculated Kitaigorodskii	Calculated Dashevsky	Contribution of free translations and rotations to a real mode	Assignment
A_1	186 w	194 w	193 vw				torsional vibration
B_1	186 w	194 w	—				of amino groups
A_2	168 w	173 vw	inactive	158.90	123.70	$R_z^{II}(54) + R_y^{II}(12) + R_x^{II}(10)$	$R_z^{II}, R_y^{II}, R_x^{II}$
B_2	167 w	174 w	—	159.17	123.80	$R_z^{II}(54) + R_y^{II}(12) + T_a^{II}(17)$	$R_z^{II}, R_y^{II}, T_a^{II}$
A_1	168 w	174 w	173 w	156.19	119.63	$R_x^{I}(49) + R_z^{II}(29)$	R_z^{I}, R_z^{II}
B_1	—	—	—	155.06	118.70	$R_x^{I}(44) + R_z^{II}(34)$	R_z^{I}, R_z^{II}
A_2	~143	153 s	inactive	155.38	107.89	$R_y^{I}(74) + T_a^{I}(10)$	R_y^{I}, T_a^{I}
B_2	~144	155 s	155 w	154.59	108.34	$R_y^{I}(74) + T_a^{I}(13)$	R_y^{I}, T_a^{I}
B_1	~143	152 m	—	148.93	98.90	$R_y^{I}(77) + R_z^{I}(10)$	R_y^{I}, R_z^{I}
A_1	~144	154 s	153 mw	148.28	100.62	$R_y^{I}(90)$	R_y^{I}
A_1	138 vw	146 vs	145 wb				torsional
B_1	~138	146 vs	—				vibration of
B_2	~138	146 vs	145 mw				methyl
A_2	138 w	146 vs	inactive				groups
A_2	128 sb	140 s	inactive	138.74	109.81	$R_z^{I}(37) + T_a^{I}(16) + R_y^{I}(10)$	$R_z^{I}, T_a^{I}, R_y^{I}$
B_2	127 w	139 w	140 w	139.84	109.70	$R_z^{I}(34) + T_a^{I}(15) + T_a^{II}(14) + T_c^{I}(10) + R_y^{I}(12)$	$R_z^{I}, T_a^{I}, T_a^{II}, T_c^{I}, R_y^{I}$
A_1	120 vsb	127 vs	127 w	134.88	108.54	$R_z^{II}(35) + R_z^{II}(19) + R_y^{II}(10)$	$R_z^{II}, R_x^{II}, R_y^{II}$
B_1	126 vsb	141 mw	—	133.13	110.17	$R_z^{II}(28) + R_z^{II}(21) + R_y^{I}(12)$	$R_z^{II}, R_x^{II}, R_y^{I}$
A_2	—	—	inactive	131.91	100.00	$R_y^{II}(30) + T_a^{II}(28) + T_a^{I}(18) + T_c^{II}(15)$	$R_y^{II}, T_a^{II}, T_a^{I}, T_c^{II}$
B_2	—	—	—	131.02	90.43	$R_y^{II}(44) + T_{-c}^{II}(15) + T_{-a}^{II}(27)$	$R_y^{II}, T_c^{II}, T_a^{II}$
B_2	107 sb	117 mb	117 mw	112.40	90.53	$R_y^{II}(40) + R_z^{II}(34) + T_c^{II}(13) + T_a^{II}(12)$	$R_y^{II}, R_z^{II}, T_c^{II}, T_a^{II}$
A_2	101 mb	112 wb	inactive	117.80	87.73	$R_y^{II}(42) + R_x^{I}(33) + T_a^{I}(21)$	$R_y^{II}, R_z^{I}, T_a^{I}$
B_1	100 sb	106 mb	—	113.36	83.75	$R_y^{II}(90)$	R_y^{II}
A_1	105 sb	116 s	117 mw	111.15	82.07	$R_y^{II}(89)$	R_y^{II}

B_2	—	—	—	120.16	83.40	$R_z^{\mathrm{I}}(36) + T_a^{\mathrm{I}}(34) + R_x^{\mathrm{I}}(11) + T_c^{\mathrm{I}}(10)$	R_z^{I}, T_a^{I}, R_x^{I}, T_c^{I}
A_2	106 vw	117 mb	inactive	111.75	83.15	$R_z^{\mathrm{II}}(30) + R_y^{\mathrm{II}}(29) + T_c^{\mathrm{II}}(15) + T_a^{\mathrm{II}}(11)$	R_z^{II}, R_y^{II}, T_c^{II}, T_a^{II}
B_1	106 w	—	—	94.43	65.98	$T_b^{\mathrm{II}}(57) + T_b^{\mathrm{I}}(13)$	T_b^{II}, T_b^{I}
A_1	100 vw	—	108 mw	95.47	70.06	$T_{-b}^{\mathrm{II}}(30) + T_c'^{\mathrm{I}}(22) + T_{-c}'^{\mathrm{II}}(22)$	T_b^{II}, T_c'
B_1	—	—	—	85.74	63.85	$R_x^{\mathrm{II}}(34) + R_x^{\mathrm{I}}(28) + T_c^{\mathrm{I}}(10)$	R_x^{II}, R_x^{I}, T_c^{I}
B_2	89 w	99 vw	99 w	86.36	62.45	$R_x^{\mathrm{I}}(64) + R_x^{\mathrm{II}}(15) + T_a^{\mathrm{I}}(13)$	R_x^{I}, R_x^{II}, T_a^{I}
A_1	88 vw	104 wb	—	85.74	62.14	$T_{-b}^{\mathrm{II}}(44) + R_x^{\mathrm{I}}(20)$	T_b^{II}, R_x^{I}
B_1	75 w	81 s	—	79.92	58.26	$T_{-b}^{\mathrm{I}}(46) + T_b^{\mathrm{II}}(28)$	T_b^{I}, T_b^{II}
A_1	74 s	80 s	80 w	82.16	59.88	$T_b^{\mathrm{I}}(70) + T_b^{\mathrm{II}}(11)$	T_b^{I}, T_b^{II}
A_2	74 w	81 mb	inactive	85.04	62.87	$R_x^{\mathrm{I}}(40) + T_{-c}^{\mathrm{I}}(22) + T_a^{\mathrm{I}}(18)$	R_x^{I}, T_c^{I}, T_a^{I}
A_2	67 w	72 mb	inactive	79.60	59.12	$T_c^{\mathrm{I}}(33) + R_x^{\mathrm{I}}(29) + T_a^{\mathrm{II}}(14) + T_c^{\mathrm{II}}(10) + R_x^{\mathrm{II}}(10)$	T_c^{I}, R_x^{I}, T_a^{II}, T_c^{II}, R_x^{II}
B_2	—	—	—	76.58	57.65	$T_{-c}^{\mathrm{I}}(56) + T_a^{\mathrm{I}}(16) + R_x^{\mathrm{I}}(11)$	T_c^{I}, T_a^{I}, R_x^{I}
A_1	66 s	73 w	77 w	73.20	54.98	$R_x^{\mathrm{II}}(35) + T_b^{\mathrm{I}}(25) + T_c'^{\mathrm{I}}(15) + T_{-c}'^{\mathrm{II}}(15)$	R_x^{II}, T_b^{I}, T_c'
B_1	63 w	72 w	—	69.55	52.69	$T_{-a}'^{\mathrm{I}}(21) + T_a^{\mathrm{II}\prime}(21) + T_c^{\mathrm{II}}(13) + T_c^{\mathrm{I}}(12) + T_b^{\mathrm{I}}(11) + T_b^{\mathrm{II}}(10)$	T_a', T_c^{II}, T_c^{I}, T_b^{I}, T_b^{II}
B_2	~55	63 s	63 ms	72.98	53.68	$R_x^{\mathrm{II}}(38) + R_z^{\mathrm{I}}(22) + R_x^{\mathrm{I}}(14)$	R_x^{II}, R_z^{I}, R_x^{I}
A_2	54 ms	61 s	inactive	77.90	56.93	$R_x^{\mathrm{II}}(40) + R_z^{\mathrm{I}}(23) + R_x^{\mathrm{I}}(13)$	R_x^{II}, R_z^{I}, R_x^{I}
B_1	53 m	63 m	—	63.97	46.53	$R_x^{\mathrm{I}}(46) + R_z^{\mathrm{I}}(24) + R_x^{\mathrm{II}}(12)$	R_x^{I}, R_z^{I}, R_x^{II}
A_1	54 vs	62 s	62 m	61.01	45.18	$R_x^{\mathrm{I}}(36) + R_x^{\mathrm{II}}(24) + R_z^{\mathrm{I}}(18) + R_z^{\mathrm{II}}(11)$	R_x^{I}, R_x^{II}, R_z^{I}, R_z^{II}
B_2	49 sb	53 s	51 w	55.20	42.38	$T_{-c}^{\mathrm{II}}(48) + R_x^{\mathrm{II}}(21) + T_a^{\mathrm{I}}(13)$	T_c^{II}, R_x^{II}, T_a^{I}
A_1	46 vs	52 vs	50 vw	48.54	37.99	$T_a^{\mathrm{I}}(43) + T_a^{\mathrm{II}}(23) + R_z^{\mathrm{I}}(12)$	T_a^{I}, T_a^{II}, R_z^{I}
B_1	45 s	53 vs	—	52.84	40.23	$T_{-c}^{\mathrm{II}}(41) + R_x^{\mathrm{II}}(22) + T_a'^{\mathrm{I}}(11) + T_{-a}'^{\mathrm{II}}(11)$	T_c^{II}, R_x^{II}, T_a'
A_2	44 ms	52 vs	inactive	50.76	40.22	$T_c^{\mathrm{II}}(47) + R_x^{\mathrm{II}}(23) + T_a^{\mathrm{II}}(10)$	T_c^{II}, R_x^{II}, T_a^{II}
B_1	34 ms	40 m	—	39.33	31.64	$T_c^{\mathrm{I}}(59) + T_{-c}^{\mathrm{II}}(31)$	T_c^{I}, T_c^{II}
B_2	31 ms	34 w	33 mw	39.76	29.24	$T_{-b}'^{\mathrm{I}}(43) + T_b^{\mathrm{II}\prime}(43)$	T_b'
A_1	29 vs	33 vs	34 mw	34.39	24.31	$T_{-a}^{\mathrm{I}}(27) + T_a^{\mathrm{II}}(60)$	T_a^{I}, T_a^{II}
A_2	29 mw	33 m	inactive				component from the
B_1	29 w	34 wb	—				other orientation
A_2	21 ms	24 m	inactive	29.00	21.55	$T_b^{\mathrm{I}}(64) + T_b^{\mathrm{II}}(25)$	T_b^{I}, T_b^{II}
A_2	19 vs	20 m	inactive	24.93	17.76	$T_{-b}^{\mathrm{I}}(27) + T_b^{\mathrm{II}}(70)$	T_{-b}^{I}, T_b^{II}

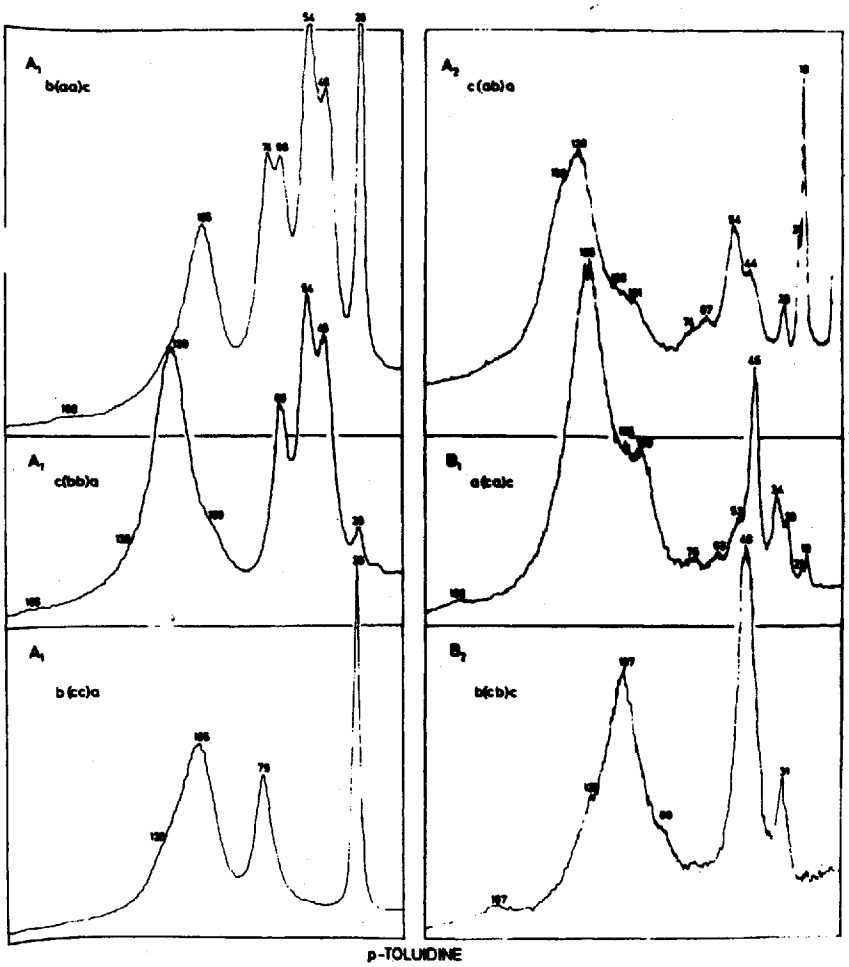

FIGURE 3 Raman spectra of paratoluidine single crystal.

where $r_{ij} = |\mathbf{r}_i - \mathbf{r}_j|$ and A, B, and α are empiric parameters determined from thermodynamic data and depending on each atom pair.

We used two sets of parameters A, B, and α. In one set we used the parameters proposed by Kitaigorodskii and his collaborators[7a–d] and in the other we employed the parameters given by Dashevsky.[8] Table III shows both sets of parameters. Only interactions at interatomic distances smaller than 4 Å were taken into account, as the contribution to the potential function at larger distances is negligible (the corresponding calculated force constants are smaller than 0.0005 mdyn/Å). By extending the limits of interactions the

TABLE III

Parameters for the Atom–Atom Interaction Potential Function

	Kitaigorodskii			Dashevsky		
Atom pair	A	B	α	A	B	α
C...C	358	42,000	3.58	474	37,700	3.52
H...H	57	42,000	4.86	21.4	9,090	4.64
C...H	154	42,000	4.12	41	14,600	4.00
N...N	259	42,000	3.78	395	76,200	4.06
N...C	308	42,640	3.68	431	50,400	3.77
N...H	109	36,200	4.25	40.6	16,200	4.33

Units of A: $\frac{\text{kcal}}{\text{mol}}$ Å^6 B: $\frac{\text{kcal}}{\text{mol}}$ α: Å^{-1}

number of atom pairs to be included increases significantly, but the calculated frequencies and eigenvectors remain almost unchanged.

Bertinotti[3] has assumed the existence of weak intermolecular hydrogen NH...N bonds at N...N distances of 3.19 Å and 3.33 Å (see Figure 1). According to this assumption molecules from different sets form infinite chains in the crystal. The chains are mutually parallel and lie along the (100) projection. Assuming that these NH...N bridges, if any, are very weak, we described them only by the stretching force constants. The values for two force constants, f_1 and f_2, for H...N bonds at distances of 2.29 and 2.40 Å, respectively, were obtained by fitting the calculated frequencies of hydrogen-bond sensitive modes to the observed bands. It was necessary to perform this fitting, since the potential function with the parameters proposed by Kitaigorodskii gave values which are too large for the corresponding force constants. Figure 4 shows the dependence of lattice modes on the value of the force constant f_1. The force constant f_2 has a fixed value chosen to give the optimal pair with f_1. Qualitatively the same diagrams were obtained for a fixed value of the force constant f_1. The force constants f_2 are given in the parentheses in Figure 4. Best agreement between the observed and calculated frequencies of the lattice modes was obtained for the pair of force constants $f_1 = 0.1$ mdyn/Å and $f_2 = 0.08$ mdyn/Å.

We should emphasize that in the calculations performed by the Dashevsky parameters A, B, and α, we were able to calculate the values of the force constants f_1 and f_2 directly from the potential function. However, comparison of the spectra calculated using the Kitaigorodskii potential function with those calculated by the Dashevsky potential function shows that in the former case the frequencies of all vibrational modes are generally higher. Even by extending the cut-off of the Dashevsky potential function the calculated frequencies could not attain the observed values.

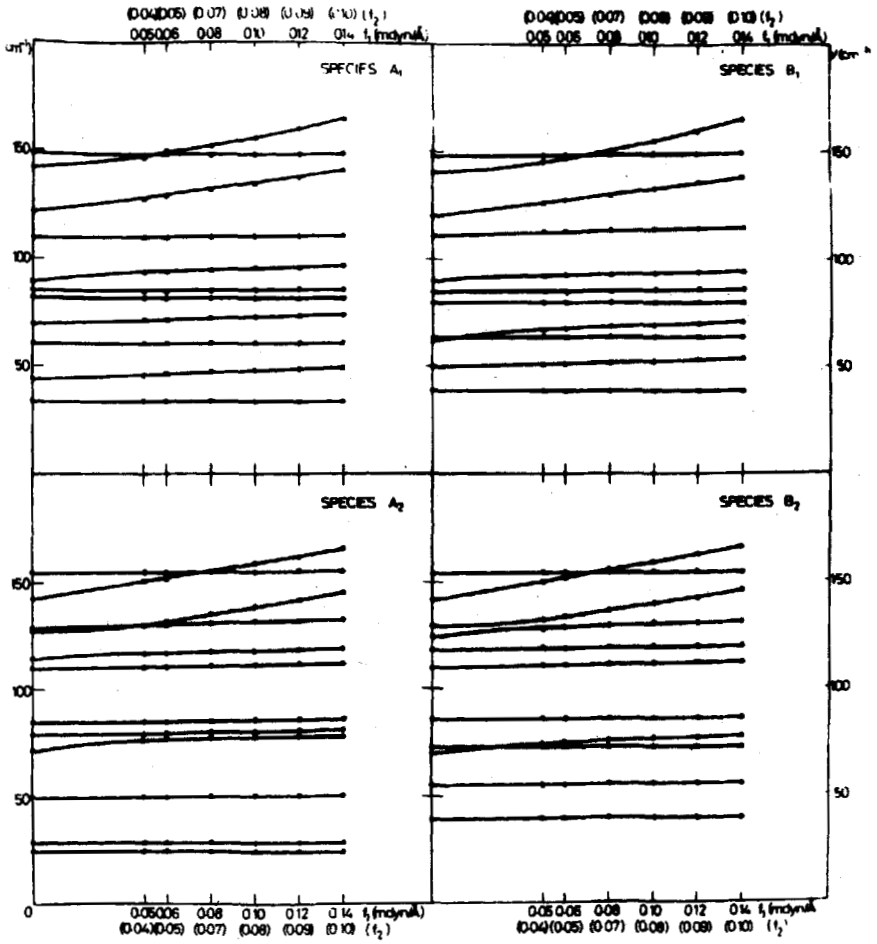

FIGURE 4 Frequency dependence on the value of the force constant f_1 corresponding to H . . . N distance equal 2.29 A.

DISCUSSION AND RESULTS

Forty lines were observed below 200 cm^{-1} in the Raman spectrum at room temperature. Frequencies for 7 additional modes were obtained by approximate extrapolation from low-temperature measurements. Table II gives the symmetry and assignment for the observed and calculated spectra. The Raman spectra observed at room temperature are given in the second

column. The intensities of the observed bands are denoted by s (strong), m (medium), and w (weak). The frequencies extrapolated from low-temperature measurements are denoted by $\sim$. The Raman spectra observed at liquid-nitrogen temperature and the far-infrared spectra observed at 34 K are given in the third and fourth columns, respectively. The results obtained by normal-coordinate analysis with both potential functions, and the best fit for the force constants f_1 and f_2 are listed in the fifth and sixth columns, respectively.

The assignment of molecular motions was performed using a component of eigenvectors for each mode. In the rigid-molecule approximation each real lattice mode is described as composed of translational (T) and rotational (R) motions of individual molecules. In the case of rotations the subscript refers to the inertial axis (see Figure 1), while in the case of translations it refers to the crystallographic axis. The superscript denotes the set of molecules contributing to the lattice mode. The contributions from free molecular rotations and translations to each lattice mode are expressed in percentages (in the parentheses). The frequencies observed in the experiment and those calculated by the Kitaigorodskii potential function are generally in reasonably good agreement. In further considerations we will refer only to this spectrum. Some of the calculated frequencies, however, exhibit a significant abberation from the corresponding observed frequencies. Possible reasons for this abberation will be discussed later.

The low symmetry of the lattice allows significant coupling between rotational and translational modes.[9] Only a certain number of modes are pure translational or pure rotational motions of symmetrically equivalent molecules.

Four bands, 138 (A_1), 137 (A_2), $\sim$137 (B_1), and $\sim$138 (B_2), of which only the first two were observed at room temperature as very weak in the Raman spectrum, and the other two were extrapolated from the low-temperature measurements, were assigned as torsional vibrations of methyl groups. This assignment is based on the assumption that the frequency of torsional vibrations of methyl groups is relatively low[10] and that the intensity of corresponding bands is weak.[11] In addition, Bougeard[11] has estimated the torsional frequency for the methyl group in hexamethylbenzene to be 117 cm^{-1}. In comparison with our case the difference in frequencies may be accounted for by the existence of six methyl groups in hexamethylbenzene. Our preliminary calculations for the internal vibrations of the paratoluidine molecule confirm the assignment we proposed.

From our preliminary calculations and the results obtained by Evans[12] for aniline, it follows that the very weak bands 186 (A_1) and 186 (B_1) might be assigned to the torsional motion of amino groups.

The coupling of torsional vibrations to rotational molecular motions,

especially to librations about the y and z axes of the molecule, is probably due to steric effects. The potential barrier to the methyl rotation in toluene was reported to be very low.[10] In paratoluidine, which is a derivative of toluene, the potential barrier is also expected to be low.

Two lines, 29 (A_2) and 29 (B_1), observed in the Raman spectrum were not assigned, since they were considered to originate from the very strong line 29 (A_1). These lines might be due either to the incorrect position of the sample in the laser beam or to the imperfections of the crystal itself.

Before interpreting our results, we wish to point out some aspects important for the dynamics of the lattice of paratoluidine. Since the molecules from the two crystallographically independent sets are linked by hydrogen bonds, the whole dynamics of the lattice is largely affected by the presence of these bonds.

The effect of van der Waals forces between molecules from different sets through methyl groups cannot be neglected, but the rigid-molecule approximation does not allow a detailed description of such interactions. Therefore, calculations in the model of a flexible molecule,[11] which would be suitable for such studies, are in progress.

It is possible to assume that strong interactions will occur between pairs of neighboring molecules from the same set, such as 1–4 or 3–2, which are symmetrical to each other with respect to the glide plane σ_b (Figure 1).

The frequencies of similar modes in the two sets are expected to be equal or very close to each other because of the similarity of the crystal field in which the molecules are situated. This may account for the grouping of bands into four very similar frequencies, often observed in the spectrum.

The lattice vibrational spectrum exhibits only one type of motion in which the two sets of molecules are completely independent. This type of motion is associated with the rotational motion of molecules about the y axis. The corresponding frequencies are $\sim$144 (A_1), $\sim$143 (B_1) for rotational motions of type R_y^{I} and 105 (A_1), 100 (B_1) for rotational motions of type R_y^{II}. This difference in energy is probably caused by the difference in length of NH ... N bridges between the amino groups of the corresponding molecules.

The energy splitting 19 (A_2) and 21 (A_2) for translational modes along the b axis can be explained in a similar manner. The excitation or nonexcitation of the vibrations in the hydrogen NH ... N bonding might cause the energy splitting in these modes. Figures 5a and b show motions specific for the T_b modes of the A_2 species. From Figure 5a it follows that the hydrogen NH ... N bonds are not excited, since the bonded molecules translate "in phase". The corresponding frequency is lower than in the case shown in Figure 5b, where the bonded molecules, and actually the two sets, move "out of phase", thus exciting all NH ... N bonds.

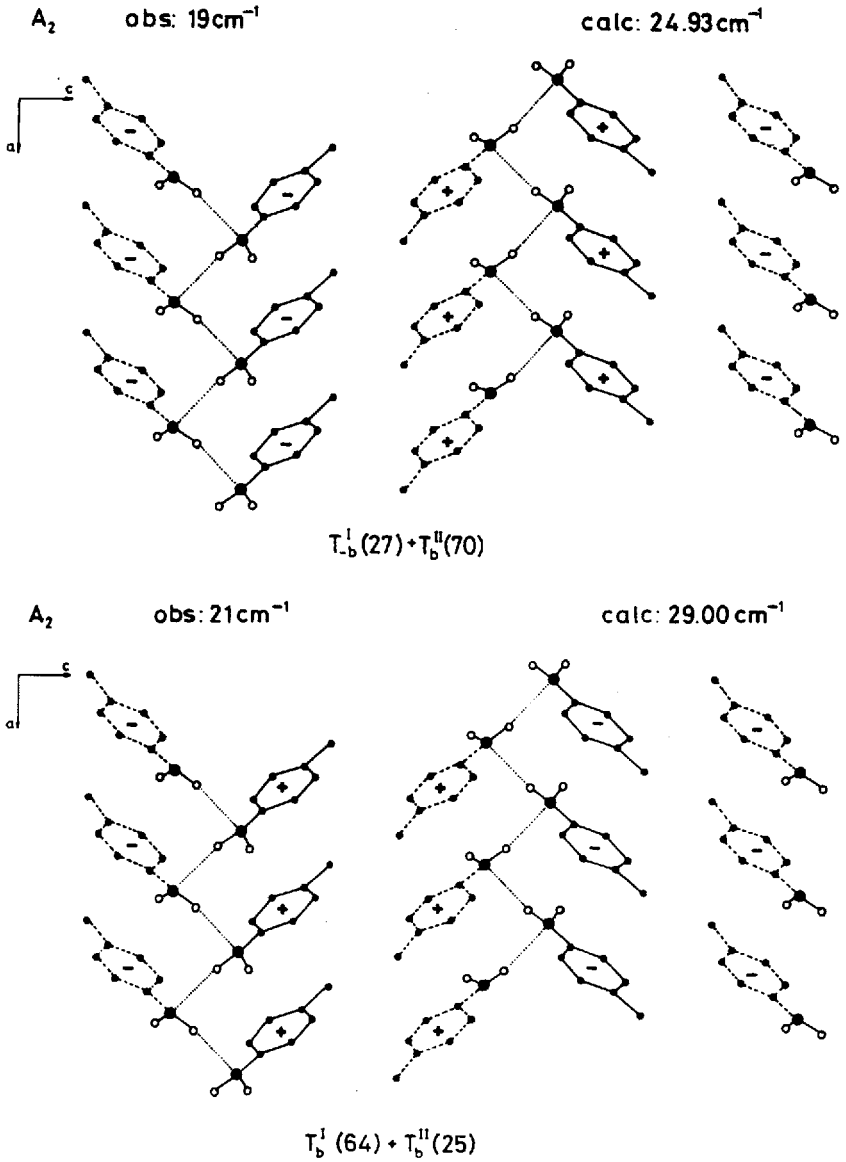

FIGURE 5a, b Hydrogen bond dependent lattice modes of paratoluidine.

It is known that the frequencies of rotational vibrations in a pure van der Waals crystal are inversely proportional to the corresponding moment of inertia.[13] The values of the moments of inertia for the paratoluidine molecule are $I_x = 429.76$, $I_y = 94.00$, and $I_z = 339.43$ (10^{-40} gr cm^2). Therefore, one might expect that the modes of highest frequencies would correspond to the rotation about the y axis. From our calculations, however, it follows that these frequencies correspond to the rotational motion about the z axis. This may be due to the existence of NH ... N bonds the vibrations of which are strongly excited in such type of motion.

A specific feature of the modes of the paratoluidine lattice are translational motions in which two rigid sets of molecules move against each other. This type of motion is due to the existence of two sets of crystallographically independent molecules. In Table II this type of motion is denoted by T'. Only the T'_b mode is relatively pure; it corresponds to the band 31 (B_2) and describes the translational motion of the two sets along the b axis. All other similar modes are coupled with other types of motion.

We have discussed only those modes which are relatively pure or which allow a simple interpretation. All other modes are complex because of the very strong coupling between rotational and translational motions from different sets, as can be seen from Table II.

Acknowledgment

The authors would like to express their gratitude to Professor B. Schrader, Institut für Theoretische Organische Chemie, Universität, Dortmund and to Professor J. P. Mathieu, Departement de Recherches Physiques, Paris for their interest and help during this work.

References

1. L. Colombo, *Spectrochim. Acta*, **23A**, 1561 (1967).
2. T. Shimanouchi and I. Harada, *J. Chem. Phys.*, **41**, 2651 (1964).
3. A. Bertinotti, *Compt. Rend.*, **127**, 4174 (1963).
   A. Bertinotti, Thèse, Paris (1965).
4. International Tables for X-Ray Crystallography, Vol. I, Symmetry Groups, Birmingham (1952).
5. T. C. Damen, S. P. S. Porto, and S. B. Tell, *Phys. Rev.*, **142**, 570 (1966).
6. D. Kirin, L. Colombo, K. Furić, and W. Meier, to be published in *Spectrochim. Acta.*

7a. A. I. Kitaigorodskii, K. V. Mirskaja, and A. B. Tobis, *Kristallografija*, **13**, 225 (1968).
b. K. V. Mirskaja and I. E. Kozlova, *Kristallografija*, **14**, 421 (1969).
c. A. I. Kitaigorodskii, K. V. Mirskaja, and V. V. Naučitelj, *Kristallografija*, **14**, 900 (1969).
d. K. V. Mirskaja and V. V. Naučitelj, *Kristallografija*, **17**, 73 (1972).

8. P. G. Dashevsky, U. T. Steruchukof, and S. A. Akappayan, *J. Struc. Chem. USSR*, **7**, 594 (1966).
9. E. B. Wilson, J. C. Decius, et P. C. Cross, *Molecular Vibrations*, McGraw-Hill, New York, 1955.
10. C. La Lau and R. G. Snyder, *Spectrochim. Acta*, **27A**, 2073 (1971).

11. D. Bougeard, P. Bleckmann, and B. Schrader, to be published.
D. Bougeard, Dissertation, Universität Dortmund (1972).
12. J. C. Evans, *Spectrochim. Acta*, **16**, 428 (1960).
13. A. Fruhling, Thèse, Paris (1950).